Short communication

Maltodextrin-powered enzymatic fuel cell through a non-natural enzymatic pathway

Zhiguang Zhu[a], Yiran Wang[a,b], Shelley D. Minteer[c], Y.-H. Percival Zhang[a,d,e,f,*]

[a] Biological Systems Engineering Department, Virginia Tech, 210-A Seitz Hall, Blacksburg, VA 24061, USA
[b] Shanghai Advanced Research Institute, Chinese Academy of Science, No. 115, Lane 572, Bibo Road, Shanghai 201203, China
[c] Chemistry Department, Saint Louis University, 3501 Laclede Avenue, St. Louis, MO 63103, USA
[d] Institute for Critical Technology and Applied Science (ICTAS), Virginia Tech, Blacksburg, VA 24061, USA
[e] DOE BioEnergy Science Center (BESC), Oak Ridge, TN 37831, USA
[f] Gate Fuels Inc, 3107 Alice Drive, Blacksburg, VA 24060, USA

ARTICLE INFO

ABSTRACT

Enzymatic fuel cells (EFCs) use a variety of fuels to generate electricity through oxidoreductase enzymes, such as oxidases or dehydrogenases, as catalysts on electrodes. We have developed a novel synthetic enzymatic pathway containing two free enzymes (maltodextrin phosphorylase and phosphoglucomutase) and one immobilized glucose-6-phosphate dehydrogenase that can utilize an oligomeric substrate maltodextrin for producing electrons mediated *via* a diaphorase and vitamin K_3 electron shuttle system. Three different enzyme immobilization approaches were compared based on electrostatic force entrapment, chemical cross-linking, and cross-linking with the aid of carbon nanotubes. At 10 mM glucose-6-phosphate (G6P) as a substrate concentration, the maximum power density of 0.06 mW cm^{-2} and retaining 42% of power output after 11 days were obtained through the method of chemical cross-linking with carbon nanotubes, approximately 6-fold and 3.5-fold better than those of the electrostatic force-based method, respectively. When changed to maltodextrin (degree of polymerization = 19) as the substrate, the EFC achieved a maximum power density of 0.085 mW cm^{-2}. With the advantages of stable, low cost, high energy density, non-inhibitor to enzymes, and environmental friendly, maltodextrin is suggested to be an ideal fuel to power enzymatic fuel cells.

© 2011 Elsevier B.V. All rights reserved.

1. Introduction

Biological fuel cells are bio-electrochemical systems that use biocatalysts rather than chemical catalysts to convert chemical energy to electrical energy directly [1,2]. Biocatalysts are less costly and biodegradable compared to costly metal catalysts. According to the classification of biocatalysts, there are two main types of biological fuel cells – enzymatic fuels (EFC) and microbial fuel cells (MFC). Compared to MFCs, EFCs are suggested to have higher power densities mainly due to better mass transfer without cellular membrane and potential higher volumetric biocatalyst loading without the dilution effect of other biomacromolecules [2–4]. Therefore, EFCs might have great potentials in powering some portable electronics in the future [1,5].

EFCs can utilize a large range of chemical compounds as fuels, including methanol, ethanol, glycerol, pyruvate, and glucose, in an increasing order of carbon number in the compounds. To increase fuel utilization efficiency, enzyme cascades are employed. Three cascade redox enzymes have been employed in an anode for complete oxidization of one-carbon methanol to CO_2 [6]. Similarly, two-carbon ethanol has been deeply oxidized for generating more electrons by using an 11-enzyme pathway [7]. Three-carbon glycerol and pyruvate have been oxidized by using two cascade dehydrogenases [8] and the enzymes in the Kreb cycle [9,10], respectively. As compared to the above relatively simple structure substrates, glucose, a six-carbon molecule, is among the cheapest organic compounds based on energy content (\$ GJ^{-1}) [11]. Therefore, a few EFCs have been developed by using glucose oxidase or glucose dehydrogenase, resulting in two electrons generated per glucose [12–14]. Currently most glucose is produced through enzymatic hydrolysis of starch, where maltodextrin is a partial hydrolysis product of starch. Different from MFCs that can utilize complicated biopolymers [15,16], starch and maltodextrin have never been used to power EFCs, to our limited knowledge. The use of maltodextrin as a chemical fuel for EFCs may offer the advantages of lower fuel costs and ~11% higher chemical energy density as compared to glucose based on fuel weight.
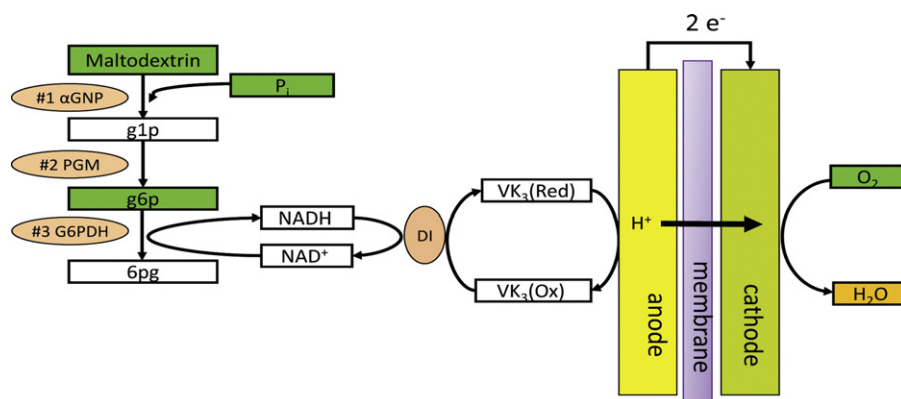
Fig. 1. Reaction scheme of the enzymatic fuel cell powered by maltodextrin or glucose-6-phosphate. (αGNP, α-glucanphosphorase; PGM, phosphoglucomutase; G6PDH, glucose-6-phosphate dehydrogenase; DI, diaphorase; g1p, glucose-1-phosphate; g6p, glucose-6-phosphate; 6pg, 6-phosphogluconate; VK$_3$, vitamin K$_3$).

Enzyme stability in EFCs can be prolonged greatly by using enzyme immobilization and/or using more stable enzymes [17]. Enzyme immobilization techniques are widely utilized in EFCs and enzyme-based biosensors, because they not only increase enzyme stability but also promote electron communication between immobilized enzymes and electrodes. Enzymes can be immobilized on the surface of electrodes through simple adsorption, entrapment, and cross-linking [18]. Simple adsorption on conductive particles, such as carbon black or graphite powder, is a common operation [13,19] but it may suffer from enzyme leakage. Entrapment of enzymes in conductive polymers can effectively prevent enzyme leakage. For example, Minteer and her coworkers have entrapped redox enzymes on electrodes by using hydrophobically modified Nafion solution casted membrane [20] or by using hydrophobically modified chitosan [21]. Scientists at Sony have entrapped enzymes using a polyion complex method based on electrostatic interactions [5]. Numerous chemical bond cross-linking techniques have been used for wiring enzymes onto the surface of electrode through redox hydrogels [22] and binding enzymes and mediators [23]. Recently large surface area and highly conductive carbon nano-tubes (CNTs) have been used in enzyme immobilization on electrodes for enhancing performances of EFCs and biosensors [24–26]. Strong chemical bonds can effectively prevent enzyme leaching and increase enzyme stability, but may also disrupt the enzymes' redox centers leading to reduced activities.

In this study, a novel three-enzyme pathway was designed to utilize maltodextrin as a fuel for enzymatic fuel cell for the first time (Fig. 1). Maltodextrin was converted to glucose-6-phosphate (G6P) by two enzymes (α-glucan (maltodextrin) phosphorylase and phosphoglucomutase) in the aqueous solution, followed by oxidation by glucose-6-phosphate dehydrogenase (G6PDH) immobilized on the anode. To enhance power output and prolong lifetime of EFCs, three different enzyme immobilization approaches were compared based on electrostatic force entrapment, cross-linking on regular carbon paper anode, and cross-linking on CNT-enhanced carbon paper anode.

2. Experimental

2.1. Reagents

All chemicals, such as glucose-6-phosphate dehydrogenase (E.C.1.1.1.49), poly-L-lysine (PLL, MW ∼70–150 kDa), diaphorase (DI, E.C.1.6.99), vitamin K$_3$ (VK$_3$), polyacrylic acid sodium salt (PAAcNa, MW ∼240 kDa), nicotinamide adenine dinucleotide (NAD$^+$), 1-(3-dimethylaminopropyl)-3-ethylcarbodiimide hydrochloride (EDC), and N-hydroxysuccinimide (NHS) were purchased from Sigma–Aldrich (St. Louis, MO) unless otherwise

mentioned. Carbon paper (AvCarb MGL200) as anode was purchased from Fuel Cell Earth (Stoneham, MA). Membrane electrode assemblies (MEAs) consisting of Nafion 212 and carbon cloth gas diffusion cathode modified with 0.5 mg cm^{-2} Pt were purchased from Fuel Cell Store (San Diego, CA). COOH-functionalized multi-walled carbon nanotubes (an outer diameter of 20–30 nm, an inner diameter of 5–10 nm, and a length of 10–30 μm) were purchased from CheapTubes.com (Brattleboro, VT). Microcrystalline cellulose (Avicel PH105) was purchased from FMC (Philadelphia, PA). Regenerated amorphous cellulose (RAC) used in enzyme purification was prepared from Avicel through its dissolution and regeneration, as described elsewhere [27].

2.2. Preparation of enzymes

The plasmids for encoding two recombinant enzymes of α-glucan-phosphorylase (αGNP, E.C.2.4.1.1) and phosphoglucomutase (PGM, E.C.2.7.5.1) were constructed as described elsewhere [28,29]. *Escherichia coli* BL21 (DE3) hosting either αGNP plasmid (pET21c-αgp) or PGM plasmid (pCIP) was grown in 200 mL of the Luria–Bertani (LB) medium supplemented with 50 μg mL^{-1} ampicillin at 37 °C. When the optical density of the cell culture at 600 nm reached ∼0.8, isopropyl β-D-1-thiogalactopyranoside (IPTG) was added to a final concentration of 0.25 mM (αGNP) followed by 4-h cell culture at 37 °C or of 1 mM (PGM) followed by 12-h cell culture at 20 °C. The cells were harvested by centrifugation and re-suspended in a 50 mM HEPES buffer (pH 7.2) containing 1 mM ethylenediaminetetraacetic acid (EDTA). After sonication and centrifugation, both enzymes were purified by RAC adsorption and intein self-cleavage method [30]. After intein self-cleavage at 37 °C for 12 h, the target protein was obtained in the supernatant of 50 mM HEPES buffer (pH 7.2). The purity of the recombinant proteins was ∼90–95% by sodium dodecyl sulfate polyacrylamide gel electrophoresis (SDS-PAGE). Their activities were measured as described previously [28,29]. αGNP was assayed at 50 °C for 5 min in 50 mM HEPES buffer (pH 7.2) containing 1 mM Mg^{2+}, 5 mM DTT, 30 mM maltodextrin, and 10 mM potassium phosphate. The enzymatic reaction was stopped by boiling and the product G1P was measured by using a glucose hexokinase/G6PDH assay kit supplemented with PGM. The activity of PGM was measured at 60 °C for 5 min in 50 mM HEPES buffer (pH 7.5) containing 5 mM Mg^{2+}, 0.5 mM Mn^{2+}, and 5 mM G1P. The product G6P was determined by using a glucose hexokinase/G6PDH assay kit.

2.3. Preparation of bioanodes

Before coated with polymer films, the L-shaped electrodes were oxidized in 2.5% K$_2$Cr$_2$O$_7$ and 10% HNO$_3$ by scanning at 5 mV s^{-1}
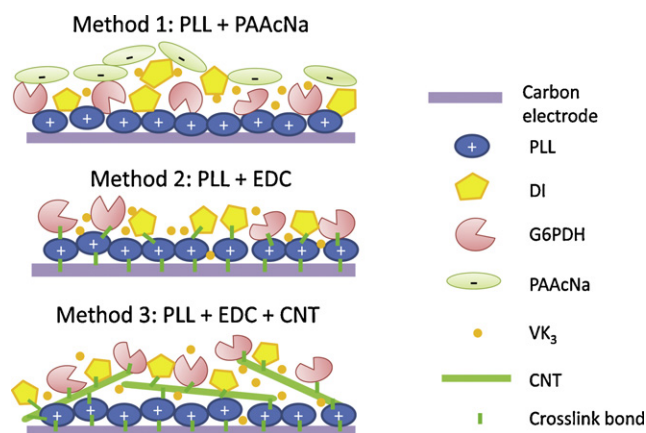
Fig. 2. Schematic layout of three immobilization methods for enzymes on anodes. Method 1: PLL+PAAcNa; Method 2: PLL+EDC; and Method 3: PLL+EDC+CNT. The various components are not drawn to scale. For example, the enzyme has a size of ~5 nm diameter; multiwalled carbon nanotubes have an outer diameter of 20–30 nm, inner diameter of 5–10 nm, and a length of 10–30 μm.

Fig. 3. Scheme of an "I-cell" set-up for this study.

from 1.55 to 1.75 V *vs.* a standard silver chloride electrode, followed by excessive water rinsing. Three enzyme immobilization methods were used to prepare bioanodes (Fig. 2). In Method 1 (PLL+PAAcNa) we modified as described previously [5]: 10 μL of a 2% (w/v) PLL solution, 10 μL of a G6PDH solution (1 U μL^{-1} in a 10 mM PBS buffer, pH 7.4, containing 0.5 mM NAD), 10 μL of a DI solution (1 U μL^{-1} in a 10 mM PBS buffer, pH 7.4), 10 μL of a 0.29 M VK$_3$ acetone solution, and 10 μL of a 0.066% (w/v) PAAcNa solution were added in the sequential order. Drying was needed at room temperature before each solution was added. The other two methods were adopted from previous reports [31–33]. In Method 2 (PLL+EDC), 10 μL of freshly prepared 24 mM EDC was added on the electrode surface. After 20 min, 10 μL of 2% (w/v) PLL solution was added and stood for 12 h. After water rinsing, another 10 μL of 400 mM EDC and 10 μL of 100 mM NHS were added on the anodes and then dried at room temperature. Ten μL of a 1 U μL^{-1} G6PDH solution and 10 μL of a 1 U μL^{-1} DI solution were added, followed by 10 μL of a VK$_3$ solution. In Method 3 (PLL+EDC+CNT), the protocols were similar to those of Method 2 except the addition of CNT on the anodes. 2.5% (w/v) CNTs suspended in a 50% ethanol solution were freshly sonicated for 30 min. After PLL coating on the electrode, 20 μL of 25 Mm EDC was further added, followed by 40 μL of CNT-containing solution deposited on the anode, and then dried at room temperature. Ten μL of 400 mM EDC and 10 μL of 100 mM NHS were added as described in Method 2. After anode preparation, the fabricated bioanodes were rinsed in water and stored in a 100 mM HEPES buffer containing 2 mM NADH and 100 mM NaNO$_3$ at 4 °C overnight before electrochemical measurements.

2.4. Electrochemical measurements

Open circuit potential and linear sweep voltammetry at a scan rate of 1 mV s^{-1} were performed at room temperature by using a CH1000B Multi-Channel Potentiostat from CH Instruments Inc. (Austin, TX). The set-up of enzymatic fuel cell (Fig. 3) was similar to the "I-cell" as described elsewhere [21]. The membrane electrode assembly including Nafion and cathode was sealed by O-rings and stacked by two glass tubes. The upper glass tube contained the enzyme buffer as the electrolyte and the lower one was empty for air-breathing. L-shaped bioanode coated with polymers and enzymes was dipped into the electrolyte when used. All the enzymes and mediators were immobilized on bioanode with the size of 1 cm^2. Nafion 212 was used as the proton exchange membrane and carbon cloth was cathode with Pt as the
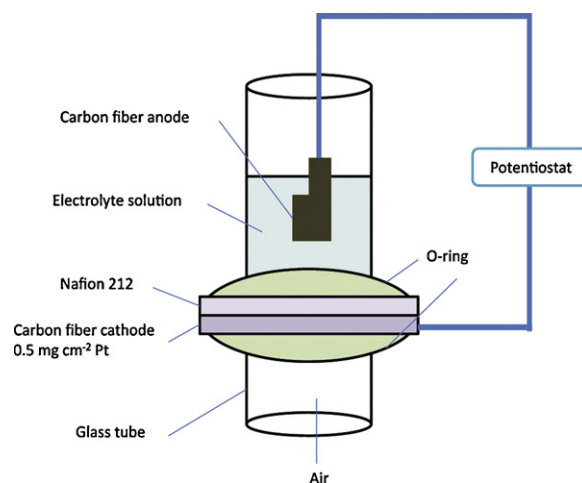
catalyst to reduce oxygen to water. The anolyte solution for comparison of three immobilization methods and checking stability of our enzymatic fuel cell system, contained 20 mM glucose-6-phosphate (G6P), 100 mM HEPES buffer (pH 7.2), 2 mM NAD, 20 mM Mg^{2+}, and 0.5 mM Mn^{2+}. The substrate concentration was also altered from 2 to 40 mM to show that the electrochemical performance increases with concentration. In cases of maltodextrin as the substrate, equivalent amount of potassium phosphate and 5 mM dichlorodiphenyltrichloroethane (DTT) were added for optimal αGNP activity, with the enzyme loading of 0.1 U mL^{-1} αGNP and 10 U mL^{-1} PGM. Polarization curves were recorded and power curves were generated by a computer equipped with software. Each experiment condition was run in triplicate and the reaction solution was replaced daily.

3. Results and discussion

Although maltodextrin may be an ideal fuel, this oligosaccharide cannot be oxidized directly by any redox enzymes. A novel synthetic enzymatic pathway was designed to contain three enzymes – αGNP, PGM, and G6PDH to utilize maltodextrin (Fig. 1). In the aqueous solution, αGNP is responsible for cleaving one anhydroglucose unit from the non-reducing end of maltodextrin plus a free phosphate ion and generating glucose-1-phosphate (G1P); and then PGM is responsible for converting G1P to G6P. The immobilized NAD-preferred G6PDH can convert G6P to 6-phosphogluconate (6PG) and generate one NADH from NAD$^+$. Two electrons from one NADH are shuttled *via* an electron transport mediator (VK$_3$) mediated by co-immobilized flavin-bound DI to the anode, as described previously [34]. VK$_3$ was chosen because of its fast kinetics and small thermodynamic loss [35]. Three different enzyme immobilization approaches were examined in the aspects of power output and lifetime of EFCs. In Method 1, the enzymes were immobilized based on electrostatic force entrapment between PLL and PAAcNa. In Methods 2 and 3, the enzymes were immobilized through crosslinking. In Method 3, CNTs were added for increasing potential power density and improving enzyme stability.

In our pathway, the first two enzymes were free in the aqueous solution for good mass transfer among the soluble substrates/soluble enzymes, and glucose-6-phosphate dehydrogenase only was immobilized on the anode. Therefore, to examine the effects of G6PDH immobilization techniques, glucose-6-phosphate was used as the substrate (Fig. 4). The result from Method 1 exhibited the highest power density of 0.01 mW cm^{-2} at a current density of 0.03 mA cm^{-2} and had a highest current density of 0.06 mA cm^{-2}.
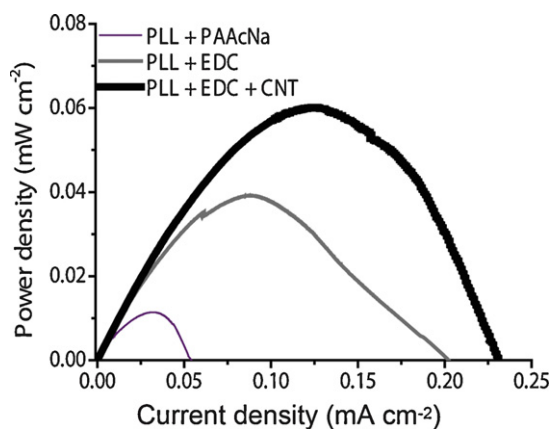
Fig. 4. Power density curves of EFCs by using three different enzyme immobilization ways. The experiments were conducted in a 100 mM HEPES buffer containing 10 mM G6P, 2 mM NAD$^+$, 20 mM Mg^{2+}, and 0.5 mM Mn^{2+} at room temperature.

The power densities of EFCs by using Method 2 and Method 3 were far higher than those by using Method 1. Method 2 had a maximum power density of 0.04 mW cm^{-2}, ~4-fold of that of Method 1. Addition of multi-walled carbon nanotubes (MWCNTs) in Method 3 further increased the maximum power density to 0.06 mW cm^{-2} at a current of 0.13 mA cm^{-2} and had a maximum current density of 0.23 mA cm^{-2}. At the same time, different enzyme immobilization techniques affected life-time of EFCs greatly (Fig. 5). Method 3 retained more power output than Methods 1 and 2. For example, Method 3 maintained 87% of power density after 2 days and 42% after 11 days, while Method 1 and 2 remained only 12% and 21% of their initial power densities in day 11, respectively. The loss of power densities with time could be mainly attributed to enzyme leaking from anode and/or the deactivation of enzymes. To overcome the first possibility, our result suggested that chemical cross-linking of enzymes with PLL modified electrode was better than electrostatic force entrapment due to stronger chemical linkages. To decrease enzyme deactivation, protein engineering and/or the use of thermostable enzyme would be chosen for prolonging enzyme lifetime in the future [36,37]. CNT's positive effects on enhanced power output was similar as reported previously [26]. One problem unsolved was the electrode modified by coating a random tangle of MWCNT could result in an unknown spatial configuration of enzymes. As shown in Fig. 2, it was difficult to control the spatial distribution of each enzyme and therefore might cause certain inefficiency in the bioanode system.
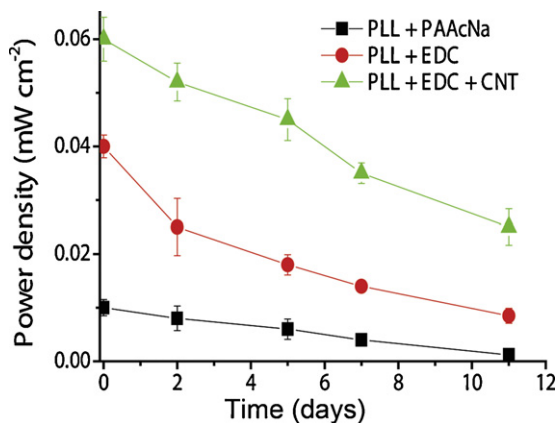

Fig. 5. Profiles of power density of EFCs in terms of time by using three different enzyme immobilization ways. The experiments were conducted in a 100 mM HEPES buffer containing 10 mM G6P, 2 mM NAD$^+$, 20 mM Mg^{2+}, and 0.5 mM Mn^{2+} at room temperature.
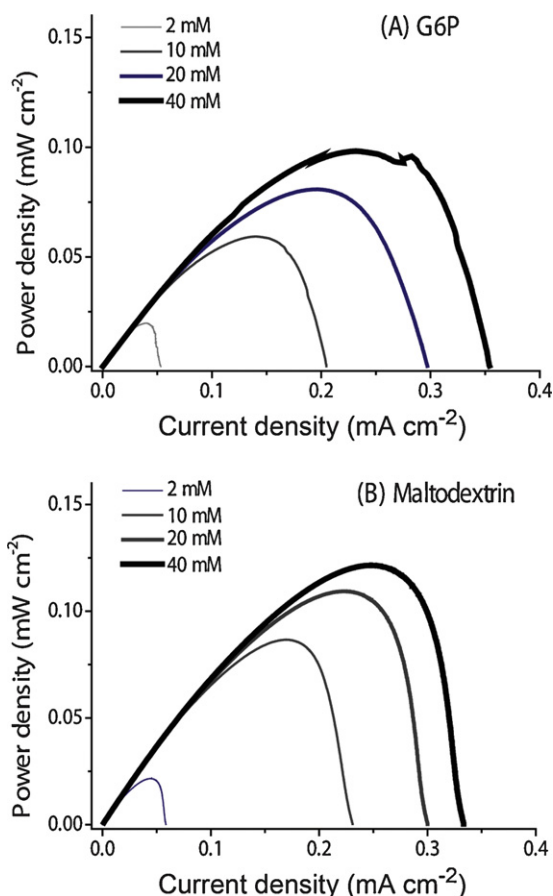

Fig. 6. Power density curves of EFCs based on Method 3 in terms of different concentration substrates of G6P (A) and maltodextrin (B). The experiments were conducted in a 100 mM HEPES buffer containing 2 mM NAD$^+$, 20 mM Mg^{2+} and 0.5 mM Mn^{2+} for G6P. When maltodextrin was substrate, the supplementary chemicals included 5 mM DTT, 0.1 U mL^{-1} αGNP, 10 U mL^{-1} PGM and various concentration KHPO$_4$/KH$_2$PO$_4$ equivalent to maltodextrin concentration at room temperature.

In addition to substrate concentration, the effects of Mg^{2+} concentration from 5 to 50 mM were studied (data not shown). Because Mg^{2+} has an important role for dehydrogenase activity but its negative impacts on proton transfer rates across the proton exchange membrane, 20 mM Mg^{2+} was chosen for the all presented experiments. Also, NaNO$_3$ addition effects on power outputs of EFCs were investigated (data not shown). Although NaNO$_3$ was thought to increase the ionic strength of the electrolyte so as to increase power output, our results showed that addition of 50–200 mM NaNO$_3$ increased power density by only 5–10% but too high NaNO$_3$ concentrations (>1 M) drastically decreased power output (data not shown). Such negative impacts may be attributed to inactivation of the enzymes (data not shown). Therefore, no NaNO$_3$ was added in the all presented experiments.

The effects of G6P and maltodextrin concentration were examined for these novel enzymatic fuel cells (Fig. 6) based on Method 3 using chemical cross-linking and CNTs for immobilization. It was found that power density increased from 0.02 to 0.1 mW cm^{-2} where G6P concentration increased from 2 to 40 mM, and highest current density moved from 0.05 mA cm^{-2} to 0.35 mA cm^{-2} (Fig. 6A). When maltodextrin was the substrate, a current density of 0.23 mA cm^{-2} and a power density of 0.085 mW cm^{-2} at 10 mM maltodextrin (Fig. 6B) were observed. An increase in maltodextrin from 2 to 40 mM led to an increase in a power density from 0.023 to 0.12 mW cm^{-2}. At the same molar concentration, EFC exhibited slightly higher power density in maltodextrin than in G6P, because

maltodextrin with an average degree of polymerization of 19 was able to release more G6P monomers per molecule. Maltodextrin is suggested to be an ideal fuel for EFCs, because it is non-volatile, less costly, and 100% biodegradable, has high solubility in water (i.e., high energy density potential), and is not an inhibitor to enzymes, as compared to commonly used fuels, such as methanol and ethanol.

The previous study conducted by Sony [5] reported very high power density of EFCs in 100 mM phosphate buffer containing 10 mM glucose, more than ten times of that by using the same enzyme immobilization technique and G6P as the substrate (Method 1, Fig. 4). A number of experiments were conducted to understand what may cause this large difference. First, it was found out that higher scanning rate of linear sweep voltammetry can result in higher current output (10 mV s^{-1}, Sony's case; 1 mV s^{-1}, this study). Second, it was found that the power output in the HEPES buffer was lower than that in the phosphate saline buffer (data not shown). Last but not least, DI used in Sony's study from *Bacillus stearothermophilus* has been reported to have a much higher activity than the one we used from *Clostridium kluyveri* [38]. This speculation will be further tested. But it was worth pointing out that Method 3 enzyme immobilization exhibited both 6-fold enhanced power output (Fig. 4) and 3.5-fold prolonged lifetime (Fig. 5), as compared to Method 1.

4. Conclusions

We have demonstrated an enzymatic fuel cell system powered by maltodextrin through a novel *in vitro* synthetic 3-enzyme pathway for the first time. A combination of chemical cross-linking between the enzymes and electrode and addition of CNT resulted in approximately 6-fold increase in maximum power density and 3.5-fold retained power output after 11 days, as compared to that where the enzyme was immobilization through entrapment. In the future, more enzymes will be brought into this system for deeper oxidization of the substrate [3,4]. For developing practical of EFCs powered by sugars, more studies will be conducted for enhancing power output and prolonging life-time, involving electrode structure, electrolyte composition, cell design, nanobiotechnology, enzyme engineering, and so on [3,39].

Acknowledgments

References

[1] S.C. Barton, J. Gallaway, P. Atanassov, Chem. Rev. 104 (2004) 4867–4886.
[2] M.J. Cooney, V. Svoboda, C. Lau, G. Martin, S.D. Minteer, Energy Environ. Sci. 1 (2008) 320–337.
[3] S.D. Minteer, B.Y. Liaw, M.J. Cooney, Curr. Opin. Biotechnol. 18 (2007) 228–234.
[4] Y.-H.P. Zhang, Biotechnol. Bioeng. 105 (2010) 663–677.
[5] H. Sakai, T. Nakagawa, Y. Tokita, T. Hatazawa, T. Ikeda, S. Tsujimura, K. Kano, Energy Environ. Sci. 2 (2009) 133–138.
[6] G.T.R. Palmore, H. Bertschy, S.H. Bergens, G.M. Whitesides, J. Electroanal. Chem. 443 (1998) 155–161.
[7] D. Sokic-Lazic, S.D. Minteer, Biosens. Bioelectron. 24 (2008) 939–944.
[8] R.L. Arechederra, B.L. Treu, S.D. Minteer, J. Power Sources 173 (2007) 156–161.
[9] D. Sokic-Lazic, S.D. Minteer, Electrochem. Solid-State Lett. 12 (2009) F26–F28.
[10] M.J. Moehlenbrock, T.K. Toby, A. Waheed, S.D. Minteer, J. Am. Chem. Soc. 132 (2010) 6288–6289.
[11] Y.-H.P. Zhang, Energy Environ. Sci. 2 (2009) 272–282.
[12] D. Sokic-Lazic, R.L. Arechederra, B.L. Treu, S.D. Minteer, Electroanalysis 22 (2010) 757–764.
[13] F. Sato, M. Togo, M.K. Islam, T. Matsue, J. Kosuge, N. Fukasaku, S. Kurosawa, M. Nishizawa, Electrochem. Commun. 7 (2005) 643–647.
[14] D. Ivnitski, B. Branch, P. Atanassov, C. Apblett, Electrochem. Commun. 8 (2006) 1204–1210.
[15] D.R. Lovley, Nat. Rev. Microbiol. 4 (2006) 497–508.
[16] B.E. Logan, Environ. Sci. Technol. 38 (2004) 160A–167A.
[17] M.J. Moehlenbrock, S.D. Minteer, Chem. Soc. Rev. 37 (2008) 1188–1196.
[18] J. Kim, H. Jia, P. Wang, Biotechnol. Adv. 24 (2006) 296–308.
[19] A. Pizzariello, M. Stred'ansky, S. Miertus, Bioelectrochemistry 56 (2002) 99–105.
[20] C.M. Moore, N.L. Akers, A.D. Hill, Z.C. Johnson, S.D. Minteer, Biomacromolecules 5 (2004) 1241–1247.
[21] T.L. Klotzbach, M. Watt, Y. Ansari, S.D. Minteer, J. Membr. Sci. 311 (2008) 81–88.
[22] V. Soukharev, N. Mano, A. Heller, J. Am. Chem. Soc. 126 (2004) 8368–8369.
[23] E. Katz, A. Riklin, V. Heleg-Shabtai, I. Willner, A.F. Buckmann, Anal. Chim. Acta 385 (1999) 45–58.
[24] R. Pauliukaite, M.E. Ghica, O. Fatibello, C.M.A. Brett, Anal. Chem. 81 (2009) 5364–5372.
[25] M.K. Wang, Y. Shen, Y. Liu, T. Wang, F. Zhao, B.F. Liu, S.J. Dong, J. Electroanal. Chem. 578 (2005) 121–127.
[26] J.J. Gooding, R. Wibowo, J.Q. Liu, W.R. Yang, D. Losic, S. Orbons, F.J. Mearns, J.G. Shapter, D.B. Hibbert, J. Am. Chem. Soc. 125 (2003) 9006–9007.
[27] Y.-H.P. Zhang, J.-B. Cui, L.R. Lynd, L.R. Kuang, Biomacromolecules 7 (2006) 644–648.
[28] X.H. Ye, Y.R. Wang, R.C. Hopkins, M.W.W. Adams, B.R. Evans, J.R. Mielenz, Y.H.P. Zhang, Chemsuschem 2 (2009) 149–152.
[29] Y. Wang, Y.-H.P. Zhang, J. Appl. Microbiol. 108 (2010) 39–46.
[30] J. Hong, Y. Wang, X. Ye, Y.-H.P. Zhang, J. Chromatogr. A 1194 (2008) 150–154.
[31] A. Vaze, N. Hussain, C. Tang, D. Leech, J. Rusling, Electrochem. Commun. 11 (2009) 2004–2007.
[32] A. Vaze, M. Parizo, J.F. Rusling, Langmuir 20 (2004) 10943–10948.
[33] A. Vaze, J.F. Rusling, J. Electrochem. Soc. 149 (2002) D193–D197.
[34] A. Sato, K. Kano, T. Ikeda, Chem. Lett. 32 (2003) 880–881.
[35] M. Togo, A. Takamura, T. Asai, H. Kaji, M. Nishizawa, Electrochim. Acta 52 (2007) 4669–4674.
[36] Y. Wang, Y.-H.P. Zhang, Microb. Cell Fact. 8 (2009) 30.
[37] W. Liu, J. Hong, D.R. Bevan, Y.-H.P. Zhang, Biotechnol. Bioeng. 103 (2009) 1087–1094.
[38] T. Sugiyama, Y. Goto, R. Matsumoto, H. Sakai, Y. Tokita, T. Hatazawa, Biosens. Bioelectron. 26 (2010) 452–457.
[39] A.K. Sarma, P. Vatsyayan, P. Goswami, S.D. Minteer, Biosens. Bioelectron. 24 (2009) 2313–2322.